Visual Transduction: A Paradigm for Signaling

E. DiBenedetto

em.diben@vanderbilt.edu

Department of Mathematics, Vanderbilt University

Nashville, TN 37240, USA

Micrograph of Salamander and Frog Retina

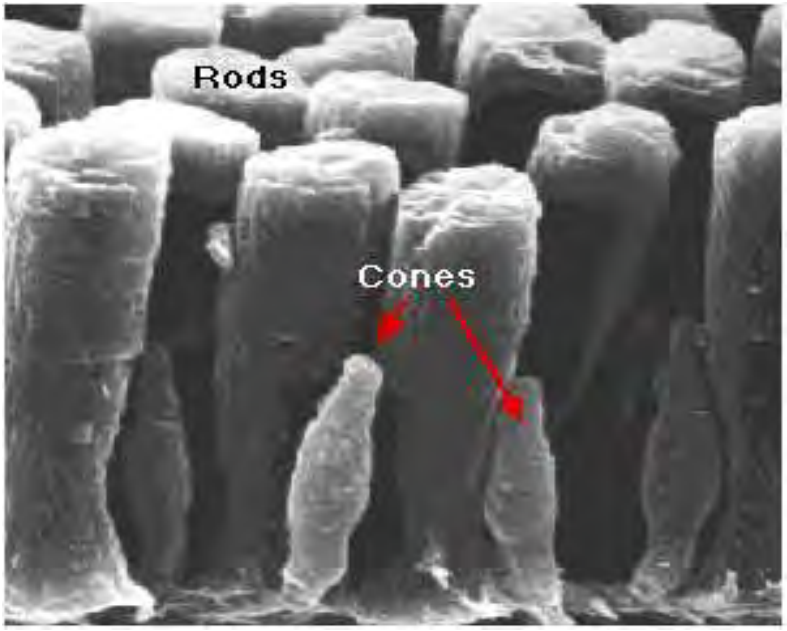

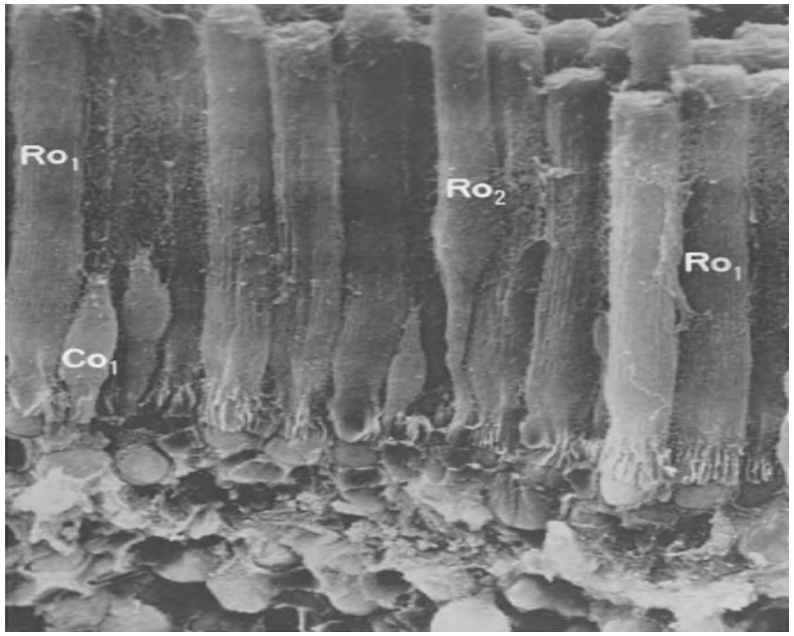

Micrograph of the Salamander Rod Outer Segment

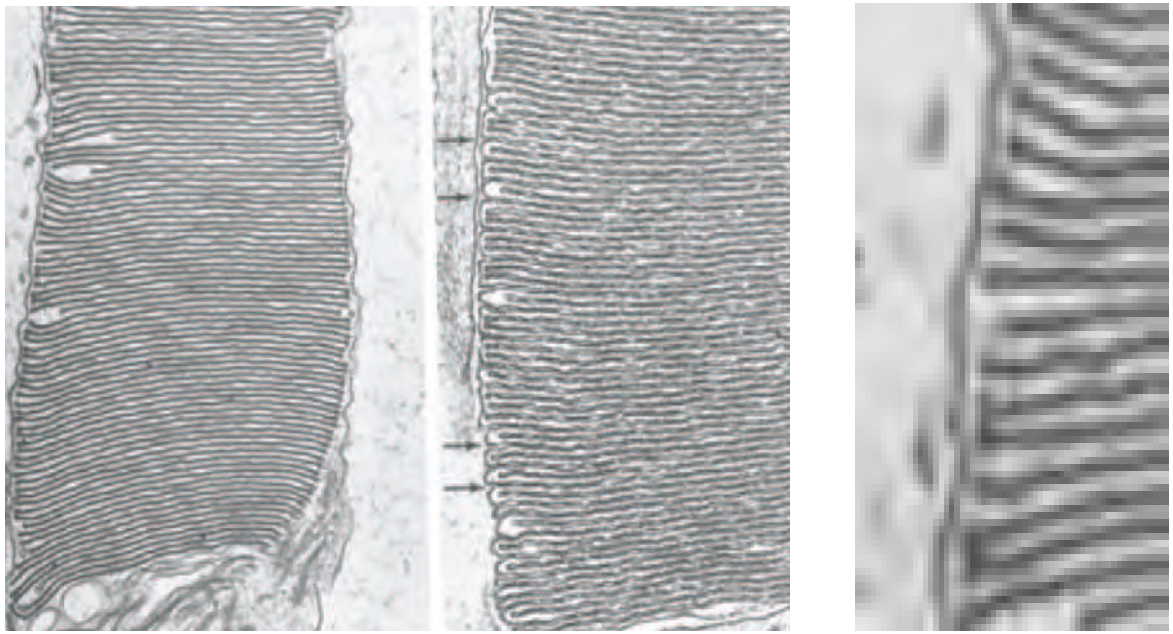

Thickness $\sigma\varepsilon_o$ of outer shell comparable to distance $\nu\varepsilon_o$ between any two discs. For the Salamander $\varepsilon_o \approx 14\,\mathrm{nm}$ and $\nu \approx \sigma \approx 1$. Here ε_o is the thickness of the "layers/discs".

Geometry of the Salamander ROS

$H \approx 22\mu\text{m}$ $R \approx 5.5\mu\text{m}$ $\varepsilon_o \approx 14\,\text{nm}$

$\nu \approx 1$ $\sigma \approx 1$ $n \approx 800$

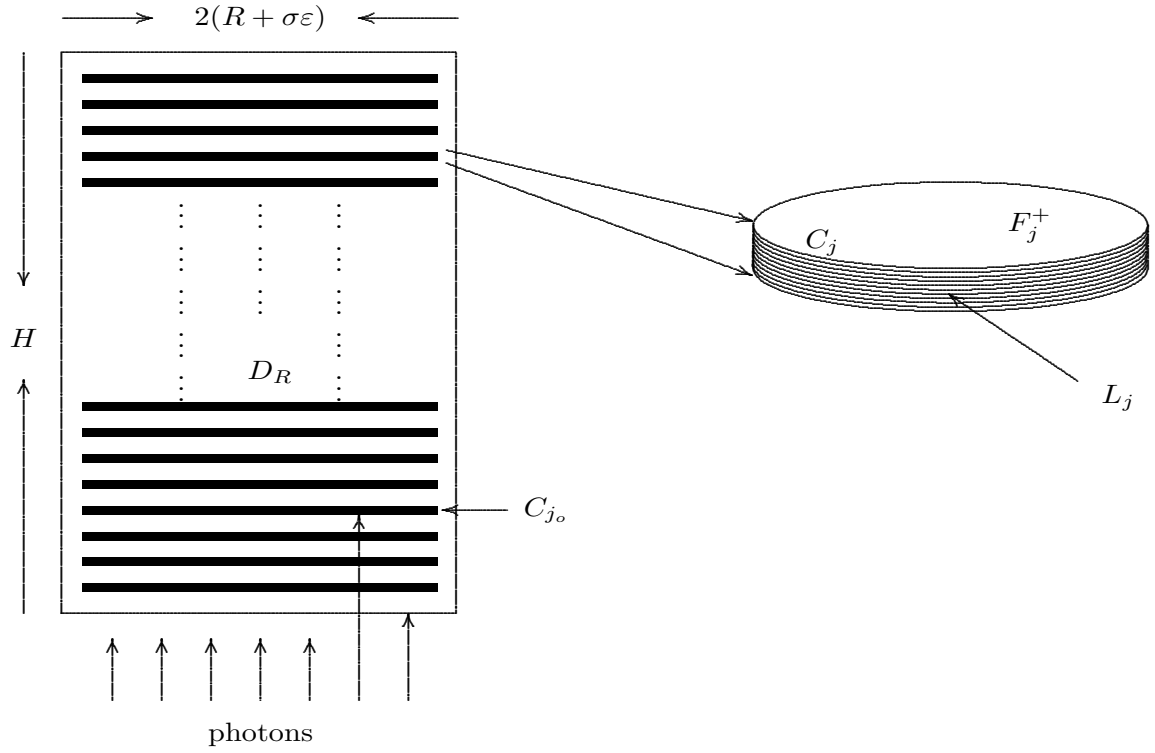

Geometry of the ROS with Incisures

$S_\varepsilon = \{D_{R+\sigma\varepsilon} - D_R\} \times (0, H)$ Outer Shell $\varepsilon \leq \varepsilon_o$

$I_j = \{\text{interdiscal spaces}\}$ thickness $\approx \nu\varepsilon$ $\nu \approx 1$

$\mathcal{B}_\varepsilon = \mathcal{V}_\varepsilon \times (0, H)$ blade-like incisures $n \approx 800$

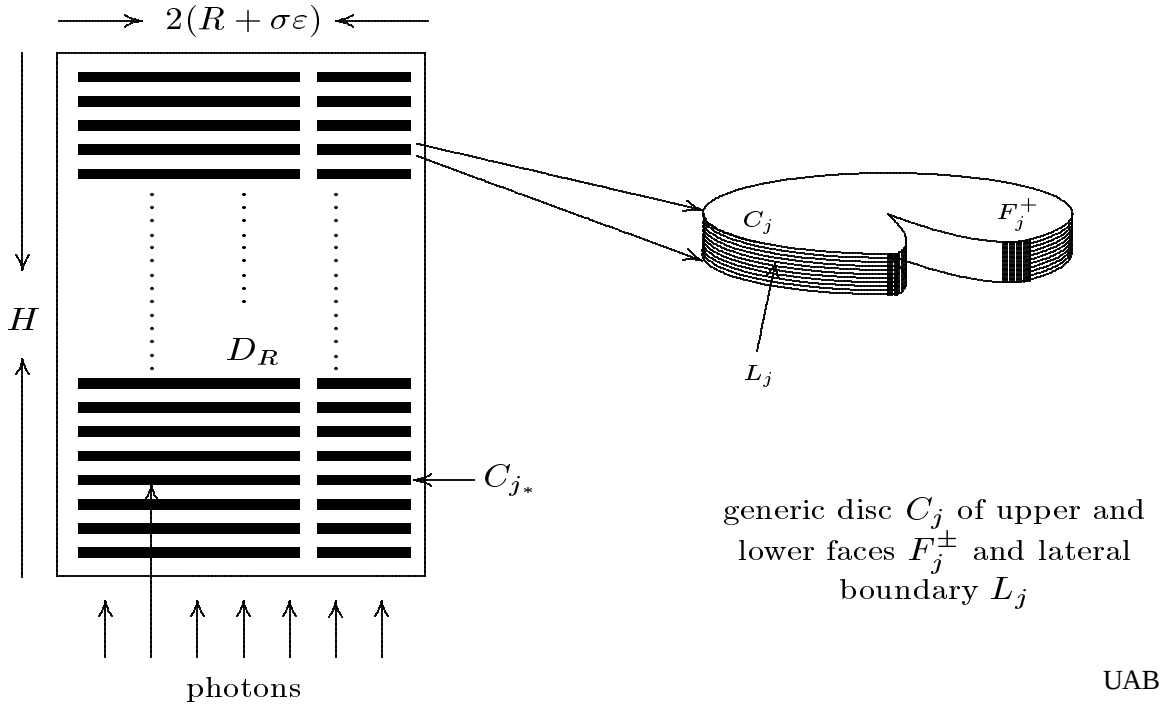

generic disc C_j of upper and lower faces $F_j^\pm$ and lateral boundary L_j

Incisures in Frog ROS

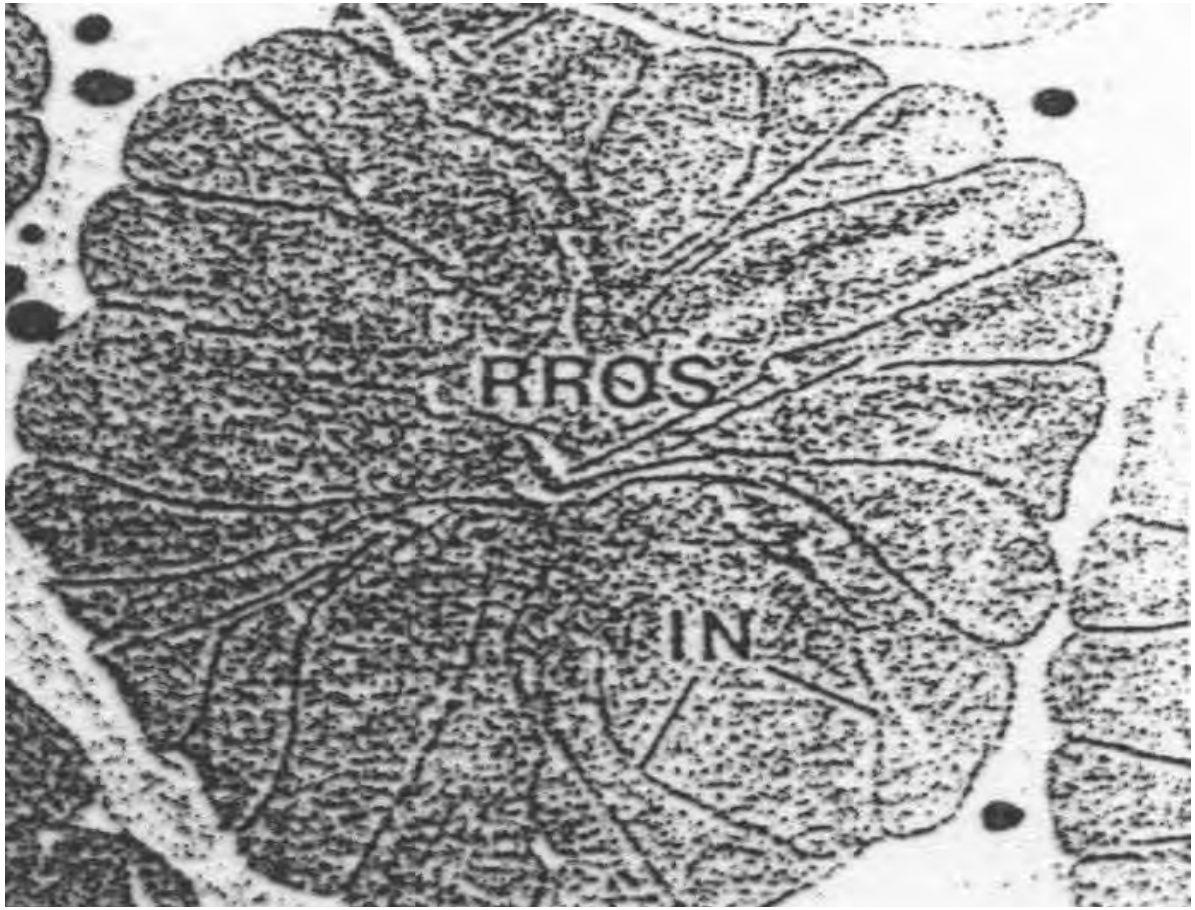

Vision Res. Vol. 22, 1982, pp. 1417–1428

Incisures in Rat ROS

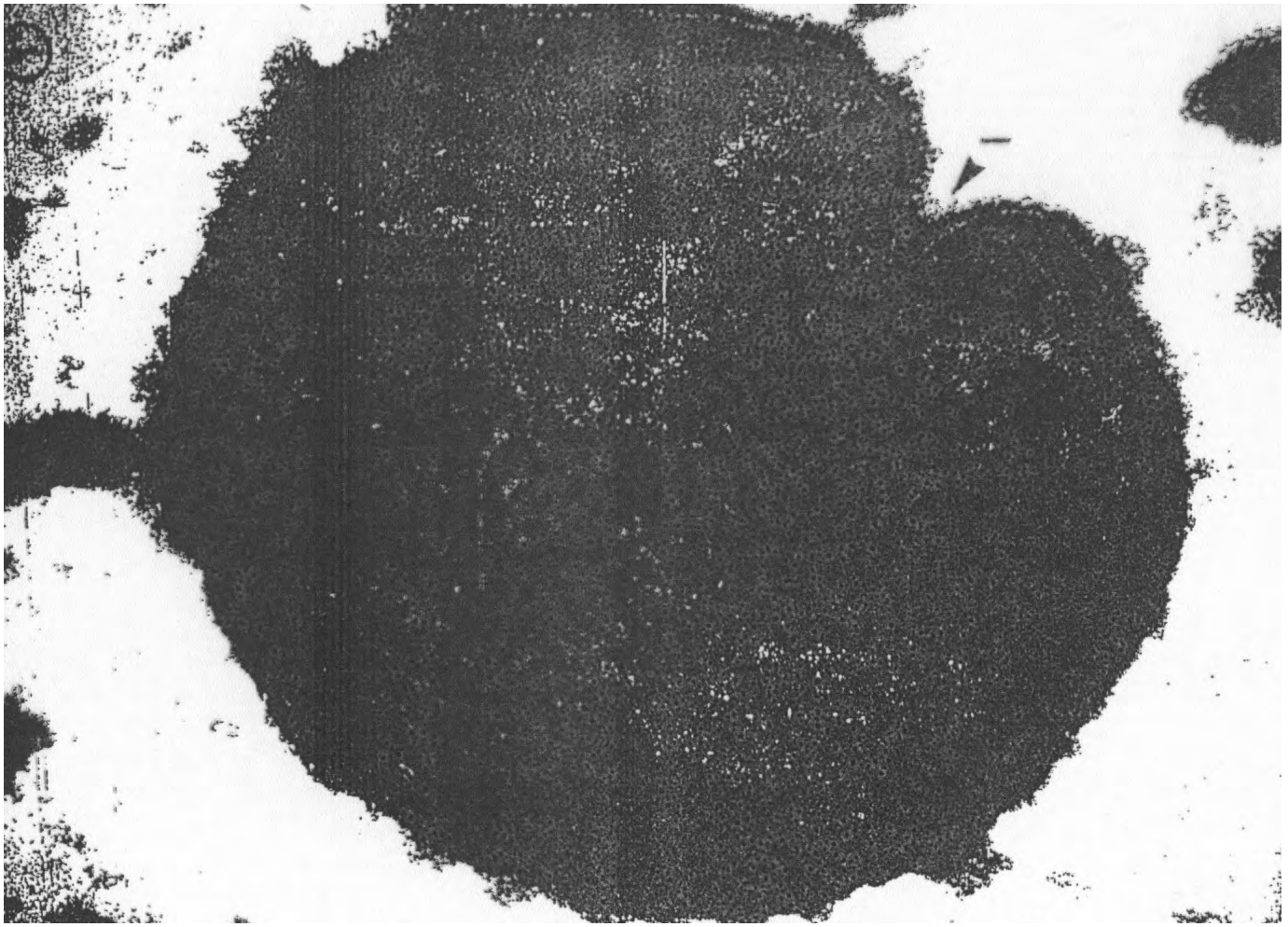

Vision Res. Vol. 7, 1967, pp. 829–836

Vision-I

- **Geometry/Anatomy is part of the System Behavior of a Biological Process**
- **Intricate Geometry Fosters Novel Mathematics**

Light Activation

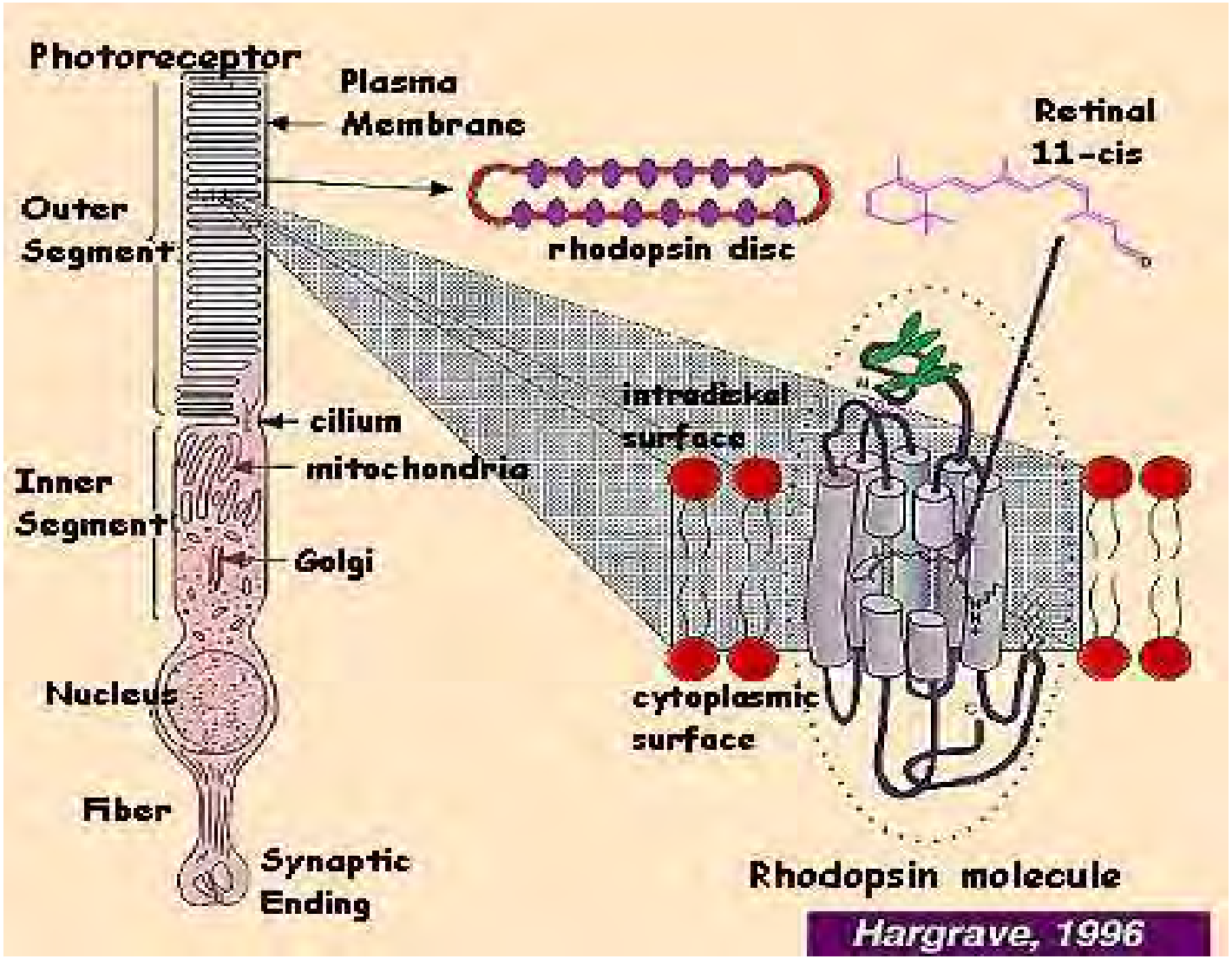

The Signaling Cascade on the Activated Disc

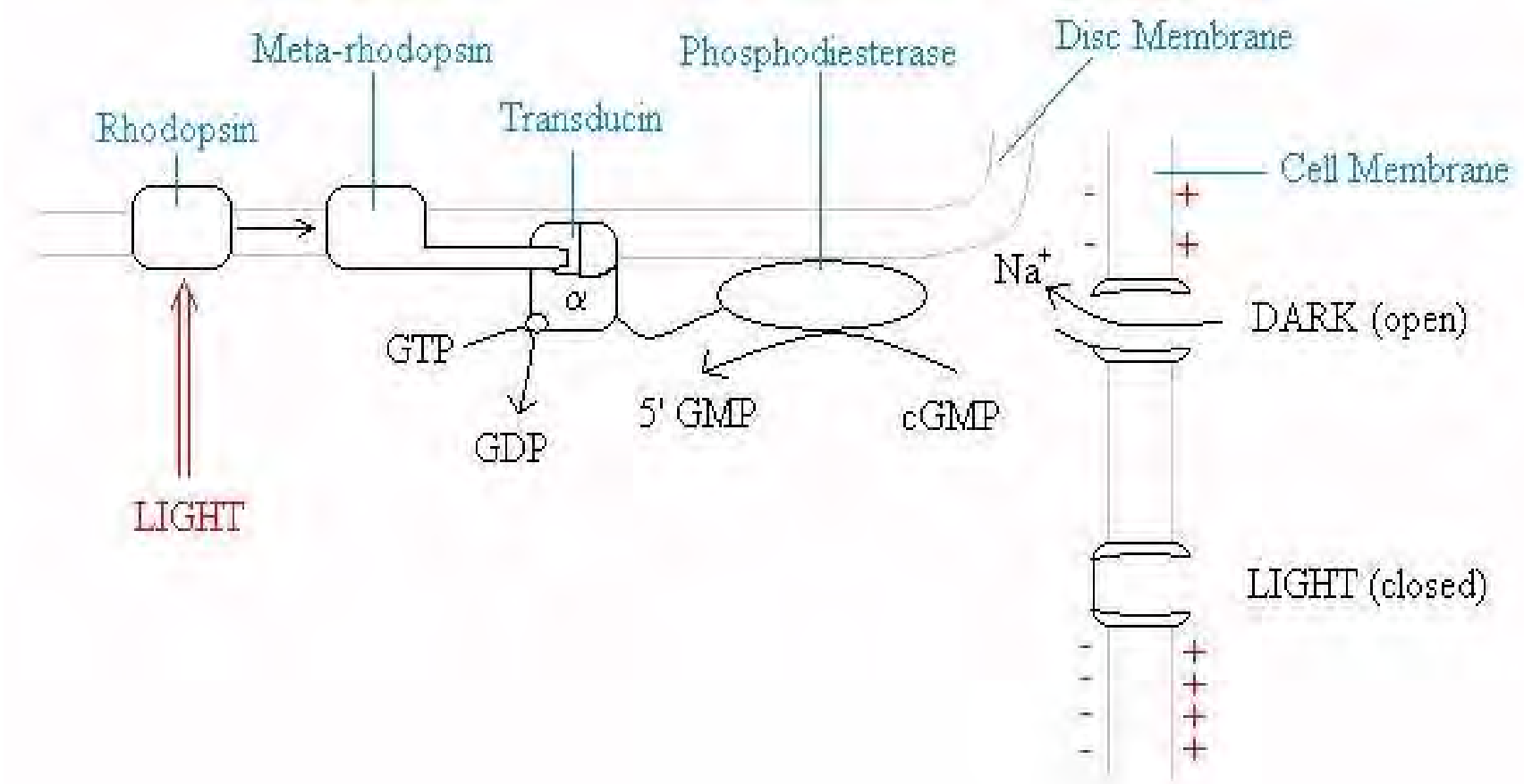

The Cascade and Resulting Photocurrent

The Cascade and Resulting Photocurrent

$$\{\text{Photon}\} \Longrightarrow \text{R} \Longrightarrow \text{R}^* \Longrightarrow \text{G} \Longrightarrow \text{G}^* \Longrightarrow \text{PDE} \Longrightarrow \text{PDE}^*$$

$$\text{depletion of cGMP} \Longrightarrow \text{closing of the channels.}$$

The Cascade and Resulting Photocurrent

$$\{\text{Photon}\} \Longrightarrow \text{R} \Longrightarrow \text{R}^* \Longrightarrow \text{G} \Longrightarrow \text{G}^* \Longrightarrow \text{PDE} \Longrightarrow \text{PDE}^*$$

$$\text{depletion of cGMP} \Longrightarrow \text{ closing of the channels.}$$

The resulting *photocurrent* generated by the cGMP–gated channels is

$$\text{J}_{\text{cG}} = \text{j}_{\text{cG}}^{\text{max}} \frac{[\text{cGMP}]^{\text{m}_{\text{cG}}}}{\text{K}_{\text{cG}}^{\text{m}_{\text{cG}}} + [\text{cGMP}]^{\text{m}_{\text{cG}}}}$$

$$\big([\text{cGMP}] = u(x,t);\ \text{m}_{\text{cG}} = 2\big).$$

The Cascade and Resulting Photocurrent

$$\{\text{Photon}\} \Longrightarrow \text{R} \Longrightarrow \text{R}^* \Longrightarrow \text{G} \Longrightarrow \text{G}^* \Longrightarrow \text{PDE} \Longrightarrow \text{PDE}^*$$

$$\text{depletion of cGMP} \Longrightarrow \text{closing of the channels.}$$

The resulting *photocurrent* generated by the cGMP–gated channels is

$$\text{J}_{\text{cG}} = \text{j}_{\text{cG}}^{\text{max}} \frac{[\text{cGMP}]^{\text{m}_{\text{cG}}}}{\text{K}_{\text{cG}}^{\text{m}_{\text{cG}}} + [\text{cGMP}]^{\text{m}_{\text{cG}}}}$$

$$\big([\text{cGMP}] = u(x,t);\ \text{m}_{\text{cG}} = 2\big).$$

NOTE: R, R^*, G, G^*, PDE, PDE^*, GC live on a "*surface*", whereas cGMP and Ca^{2+} live in a "*volume*".

Vision-II

- **Combining Biophysics, Biochemistry and Geometry/Anatomy**
- **(subtitle) System Behavior**

Revisiting the Process by Injecting 3 New Ideas

Revisiting the Process by Injecting 3 New Ideas

- **Modeling on Site (Surface to Volume)**

  PDE*–cGMP interactions should be modeled as fluxes sources on the disc surfaces. Similarly for Ca^{2+} fluxes on the outer shell.

Revisiting the Process by Injecting 3 New Ideas

- **Modeling on Site (Surface to Volume)**

  PDE^*–cGMP interactions should be modeled as fluxes sources on the disc surfaces. Similarly for Ca^{2+} fluxes on the outer shell.

- **Modeling by the Geometry**

  Domain of diffusion is *horizontally thin* (interdiscal space) and *vertically thin* (outer shell). Account for both and their interaction.

Revisiting the Process by Injecting 3 New Ideas

- **Modeling on Site (Surface to Volume)**

  PDE^*–cGMP interactions should be modeled as fluxes sources on the disc surfaces. Similarly for Ca^{2+} fluxes on the outer shell.

- **Modeling by the Geometry**

  Domain of diffusion is *horizontally thin* (interdiscal space) and *vertically thin* (outer shell). Account for both and their interaction.

- **Homogenizing and Concentrating**

  Reduce the problem to one with simpler geometry, still preserving the **same** features of the original one.

The Limit with Constant Volume Fraction

The ratio of the volume occupied by the discs $C_{\varepsilon,j}$ to the volume of $\Omega - \mathcal{B}_\varepsilon$ is kept constant as $\varepsilon \longrightarrow 0$.

$$\frac{\text{vol}\left(\bigcup_{j=1}^{n} C_{\varepsilon,j}\right)}{\text{vol}(\Omega - \mathcal{B}_\varepsilon)} = \mu_o$$

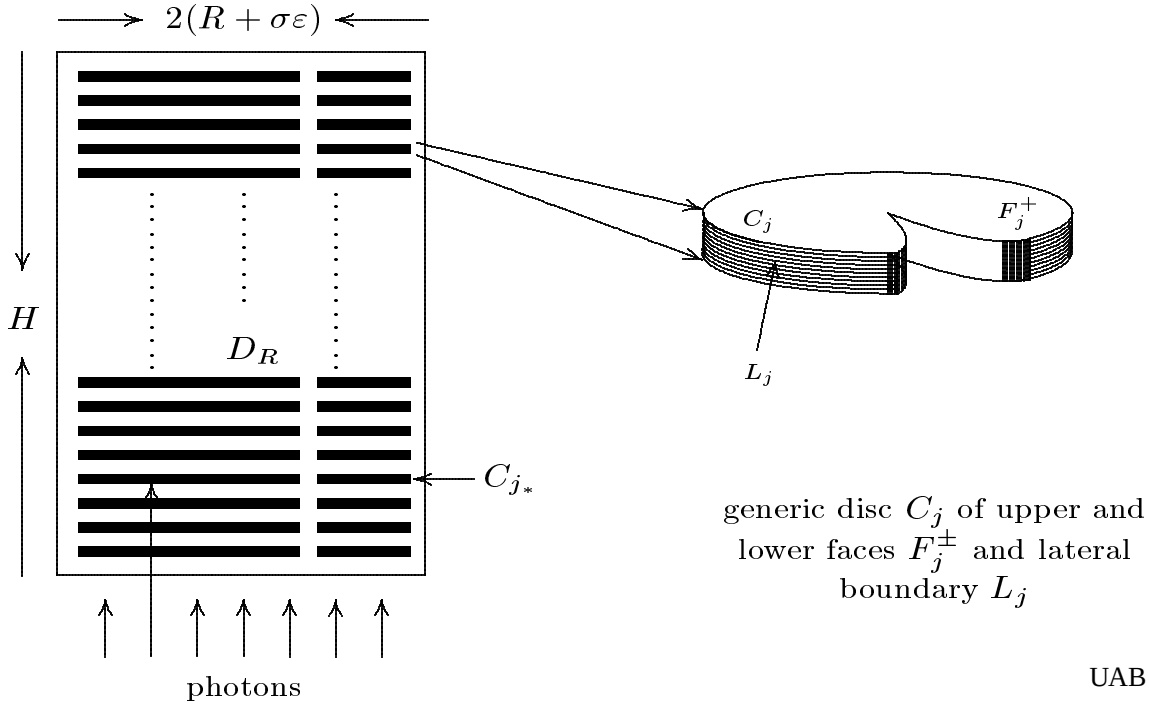

The Formal Limiting Domains-I

$$\mathcal{V}_\varepsilon \longrightarrow \mathcal{V} = \{r_o < x_1 < R\} \times \{x_2 = 0\}$$

$$D_{R+\sigma\varepsilon} - \mathcal{V}_\varepsilon \longrightarrow D_R - \mathcal{V}$$

$$D_{R+\sigma\varepsilon} - D_R \longrightarrow \partial D_R$$

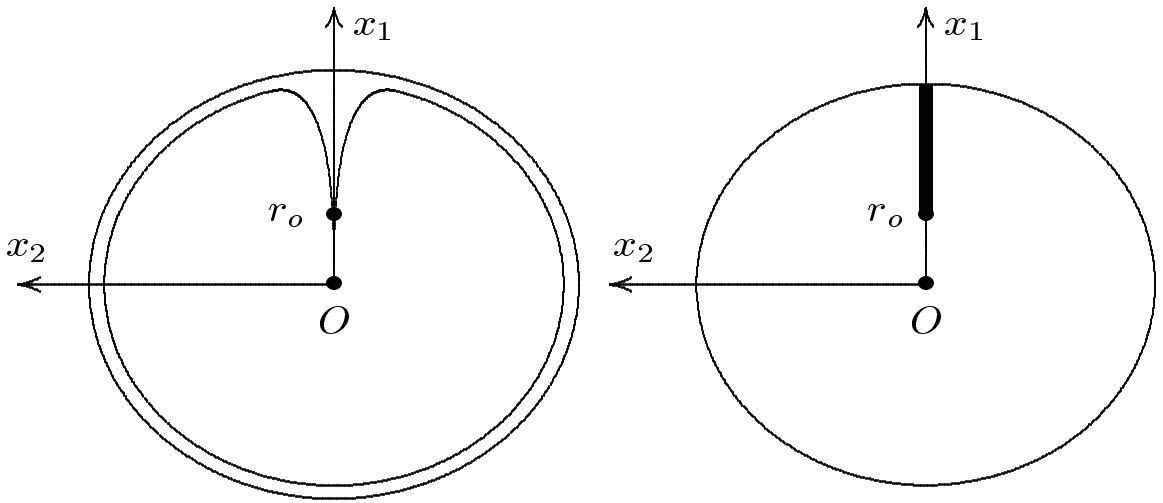

The Formal Limiting Domains-II

$$S_\varepsilon = \{D_{R+\sigma\varepsilon} - D_R\} \times (0,H) \quad \longrightarrow \quad S = \partial D_R \times (0,H)$$

$$\mathcal{B}_\varepsilon = \mathcal{V}_\varepsilon \times (0,H) \quad \longrightarrow \quad \mathcal{V} \times (0,H)$$

$$\widetilde{\Omega}_\varepsilon = \{D_{R+\sigma\varepsilon} - \mathcal{V}\varepsilon\} \times (0,H) \quad \longrightarrow \quad \Omega = \{D_R - \mathcal{V}\} \times (0,H)$$

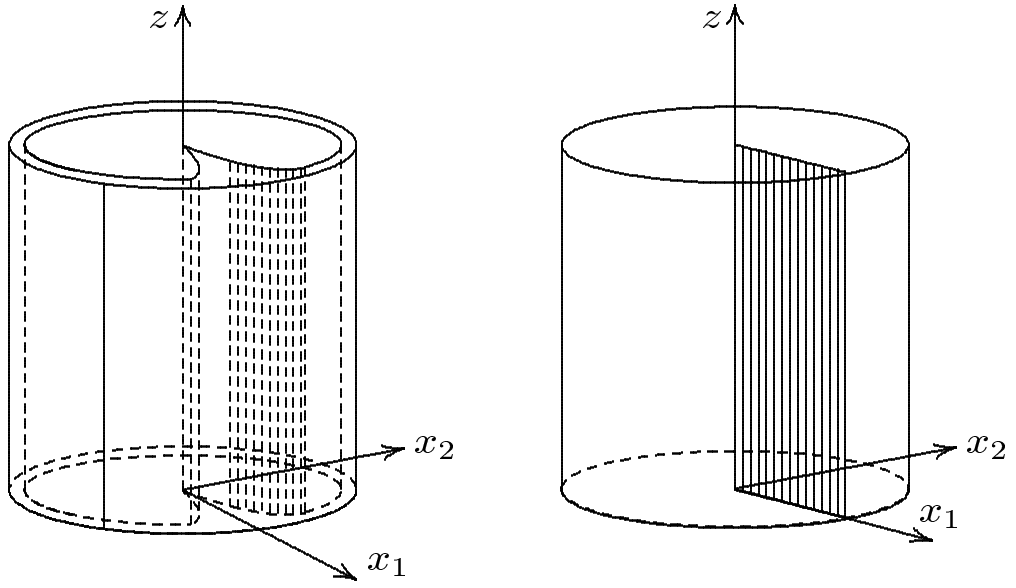

Limiting Domains and Functions as $\varepsilon \longrightarrow 0$

The approximating 2nd Messengers cGMP and Ca^{2+} (say u_ε for cGMP) tend to 3 functions each satisfying a diffusion process in its domain of definition.

Limiting Domains and Functions as $\varepsilon \longrightarrow 0$

The approximating 2nd Messengers cGMP and Ca^{2+} (say u_ε for cGMP) tend to 3 functions each satisfying a diffusion process in its domain of definition.

- $u(x, y, z, t)$ defined in the limiting cytoplasm and called the **interior limit**

Limiting Domains and Functions as $\varepsilon \longrightarrow 0$

The approximating 2nd Messengers cGMP and Ca^{2+} (say u_ε for cGMP) tend to 3 functions each satisfying a diffusion process in its domain of definition.

- $u(x, y, z, t)$ defined in the limiting cytoplasm and called the **interior limit**
- u_S defined in S and called the **limit at the outer shell**

Limiting Domains and Functions as $\varepsilon \longrightarrow 0$

The approximating 2nd Messengers cGMP and Ca^{2+} (say u_ε for cGMP) tend to 3 functions each satisfying a diffusion process in its domain of definition.

- $u(x, y, z, t)$ defined in the limiting cytoplasm and called the **interior limit**
- u_S defined in S and called the **limit at the outer shell**
- $u_{\mathcal{B}}$ defined in the limiting blade $\mathcal{B}$, and called the **limit in the incisure**

Global Weak Form

$$(1-\mu_o)\left\{\iint_{\Omega_T-\mathcal{B}_T}\{u_t\varphi+\nabla_{\bar{x}}u\cdot\nabla_{\bar{x}}\varphi+(u-f)\varphi\}dxdt\right\}_{\text{interior}}$$

$$+\sigma\varepsilon_o\left\{\iint_{S_T}\{u_{S,t}\varphi+\nabla_S u_S\cdot\nabla_S\varphi\}d\eta dt\right\}_{\text{outer shell}}$$

$$+2\left\{\iint_{\mathcal{B}_T}r\theta_{\varepsilon_o}(r)\{u_{\mathcal{B},t}\varphi+\nabla_{\mathcal{B}}u_{\mathcal{B}}\cdot\nabla_{\mathcal{B}}\varphi\}drdzdt\right\}_{\text{incisure}}=0$$

valid for all testing functions $\varphi\in W^{1,2}(\bar{\Omega}_T)$ roughly speaking in the dual classes of u, $u_{\mathcal{B}}$ and u_S.

Vision-III

- **Novel Mathematics**
- **(subtitle) Partial Differential Equations in Fractured Domains or Domains with Spikes**

The form of $f(u)$ Contains the Biochemistry

The form of $f(u)$ Contains the Biochemistry

$$f([\mathrm{cGMP}]) = \tfrac{1}{2}\left\{\beta_{\mathrm{dark}}[\mathrm{cGMP}] - \frac{\alpha}{1+([\mathrm{Ca}^{2+}]/\mathrm{K}_{\mathrm{cyc}})^{\mathrm{m}_{\mathrm{cyc}}}}\right\}$$
$$- \delta_{z_*}\mathrm{k}^*_{\sigma;\mathrm{hyd}}[\mathrm{PDE}^*]_\sigma[\mathrm{cGMP}]$$

Here [cGMP] and [Ca^{2+}] are unknowns to be determined by the system of equations. [PDE^*] is a datum generated by the activation cascade. More on this later.

The form of $f(u)$ Contains the Biochemistry

$$f([\mathrm{cGMP}]) = \tfrac{1}{2}\left\{\beta_{\mathrm{dark}}[\mathrm{cGMP}] - \frac{\alpha}{1+([\mathrm{Ca}^{2+}]/\mathrm{K}_{\mathrm{cyc}})^{\mathrm{m}_{\mathrm{cyc}}}}\right\}$$
$$- \delta_{z_*}\mathrm{k}^*_{\sigma;\mathrm{hyd}}[\mathrm{PDE}^*]_\sigma[\mathrm{cGMP}]$$

Here [cGMP] and $[\mathrm{Ca}^{2+}]$ are unknowns to be determined by the system of equations. $[\mathrm{PDE}^*]$ is a datum generated by the activation cascade. More on this later.

VISION: Inform Mathematics with Biochemistry

Simulated and Experimental Current Drop $1 - J/\mathbf{j_{dark}}$

Simulated and Experimental Current Drop $1 - J/\mathbf{j_{dark}}$

- Experimental data for mouse SPR provided by F. Rieke (Seattle).

Simulated and Experimental Current Drop $1 - J/\mathbf{j_{dark}}$

- Experimental data for mouse SPR provided by F. Rieke (Seattle).

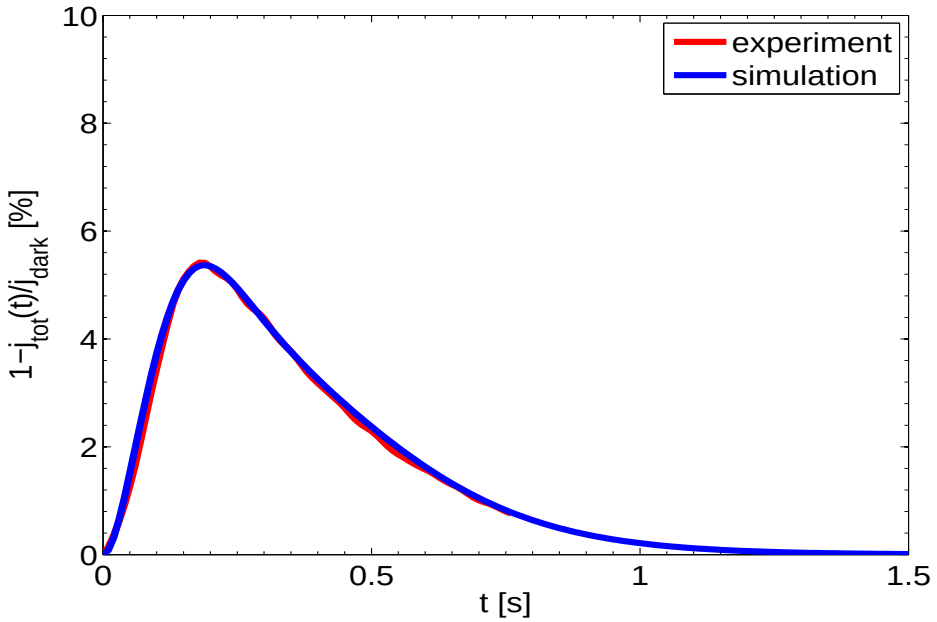

Simulated and Experimental Current Drop $1 - J/\mathbf{j_{dark}}$

- Experimental data for mouse SPR provided by F. Rieke (Seattle).

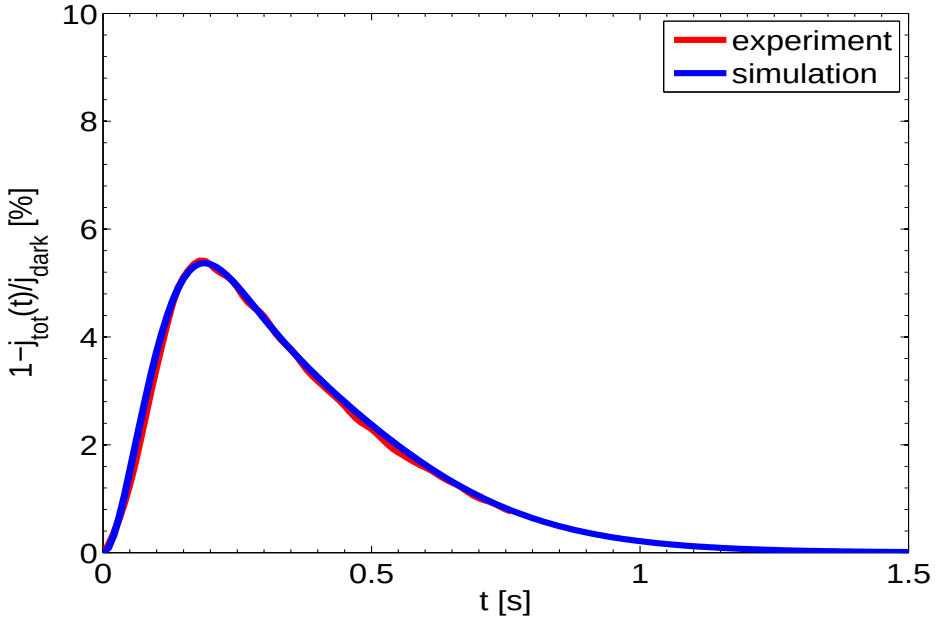

- **Full Model** (non homogenized) 8sec simulation on 20 processors of IBM series cluster (Oak Ridge Labs) took 57 hours. Same 8sec simulation with the **HM** (homogenized model) 8sec simulation took 50 seconds of an Intel Xeon

Single Photon. Current as a Function of the Incisures (Salamander)

Single Photon. Current as a Function of the Incisures (Salamander)

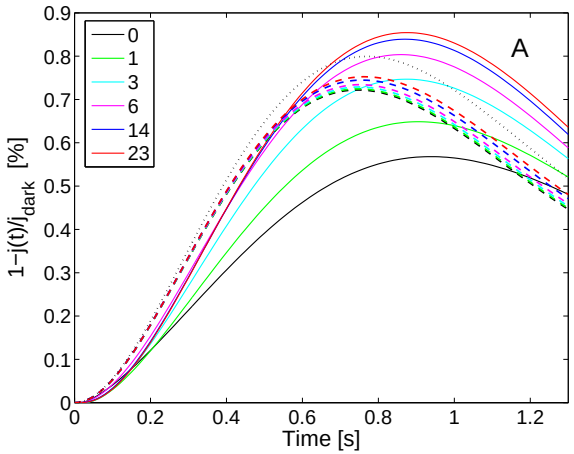

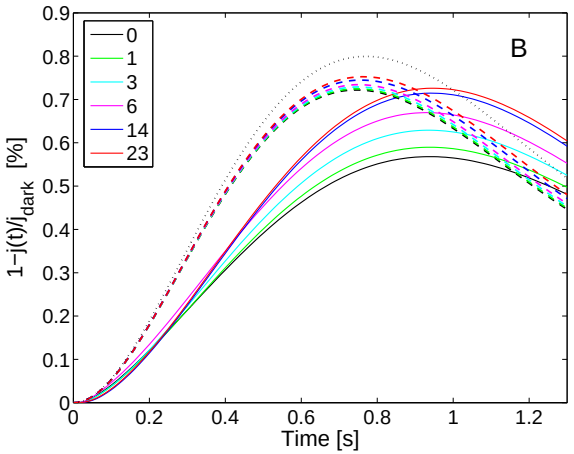

Single Photon. Current as a Function of the Incisures (Salamander)

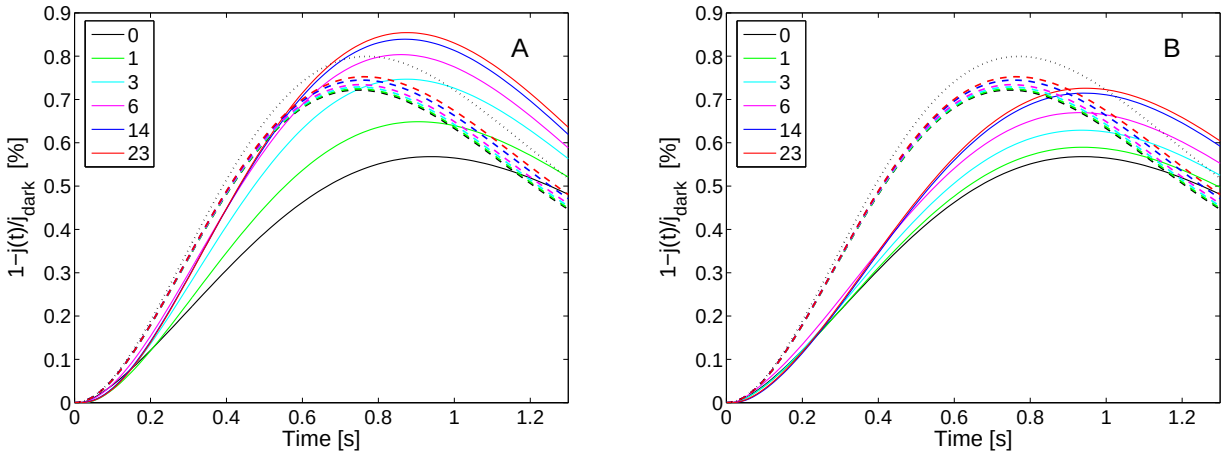

- Continuous line: tridimensional homogenized model; Dashed line: longitudinal well-stirred model; Dotted line: totally well-stirred model.

Single Photon. Current as a Function of the Incisures (Salamander)

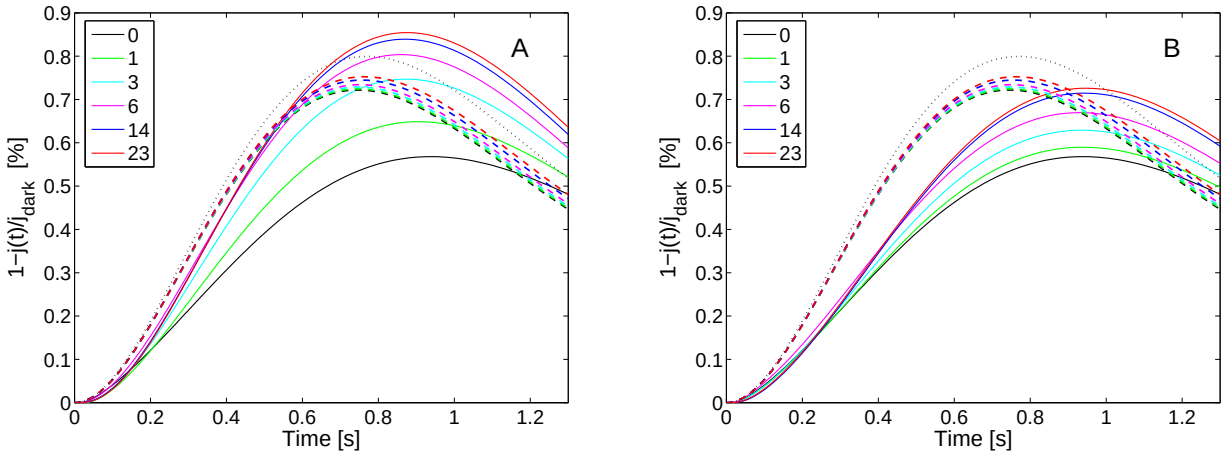

- Continuous line: tridimensional homogenized model; Dashed line: longitudinal well-stirred model; Dotted line: totally well-stirred model.
- **Panel A:** Each incisure is an isosceles triangle of base $15nm$ and height 4.64μm. There are 23 of them to reproduce total area of $\approx 0.82\mu\text{m}^2$ estimated by Olson-Pugh, 1994.

Single Photon. Current as a Function of the Incisures (Salamander)

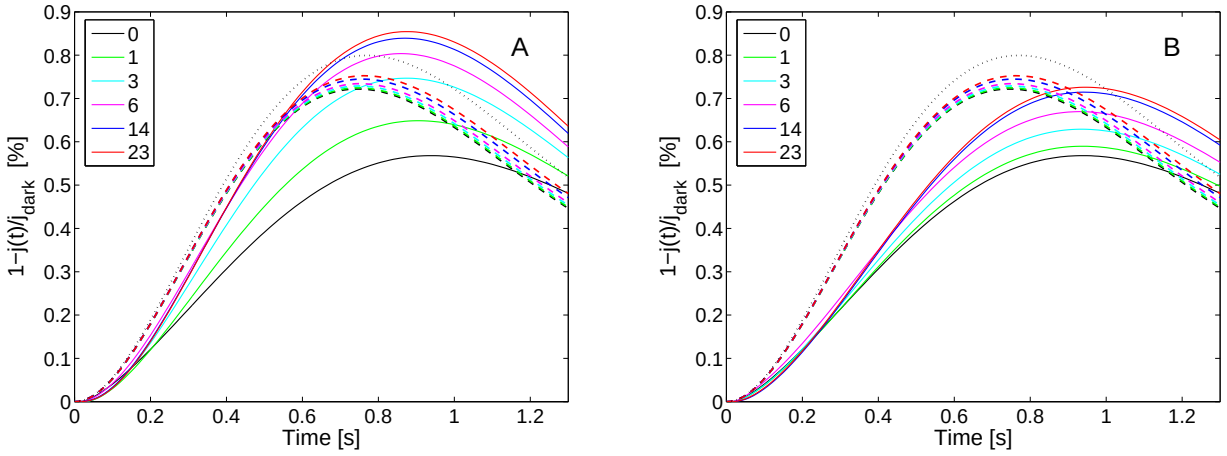

- Continuous line: tridimensional homogenized model; Dashed line: longitudinal well-stirred model; Dotted line: totally well-stirred model.
- **Panel A:** Each incisure is an isosceles triangle of base $15nm$ and height 4.64μm. There are 23 of them to reproduce total area of $\approx 0.82\mu\text{m}^2$ estimated by Olson-Pugh, 1994.
- **Panel B:** Incisures with equal area but half the length and double the width of those in the left figure (wide and short, with tip away from activation site).

Vision-IV

- **Numerical Analysis, Programming, Simulating**
- **(subtitle) Capability of Replacing Wet-Bench Experiments with Virtual Experiments**

The Activation/Deactivation Cascade, Variability and Fidelity of the SPR

The Activation/Deactivation Cascade, Variability and Fidelity of the SPR

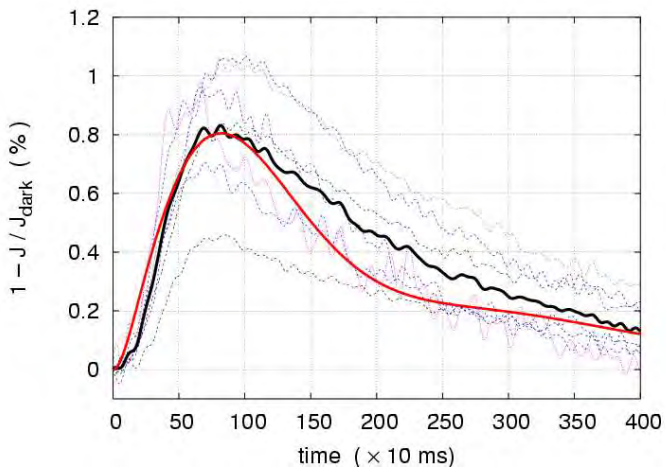

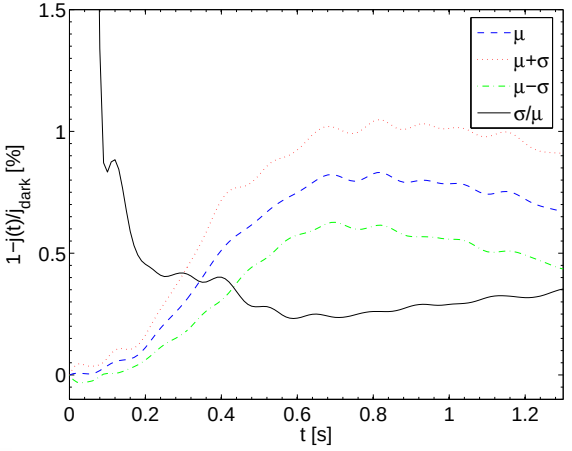

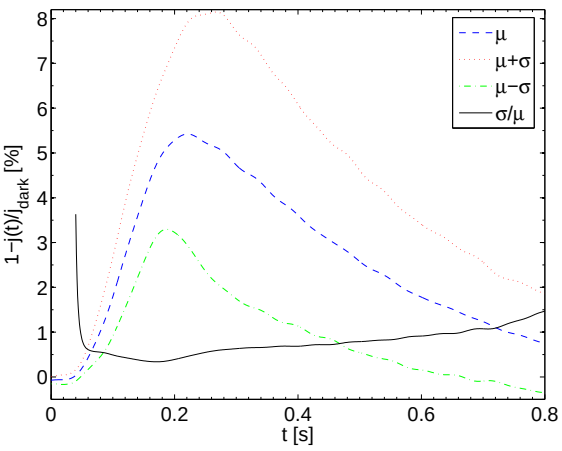

The Activation/Deactivation Cascade, Variability and Fidelity of the SPR

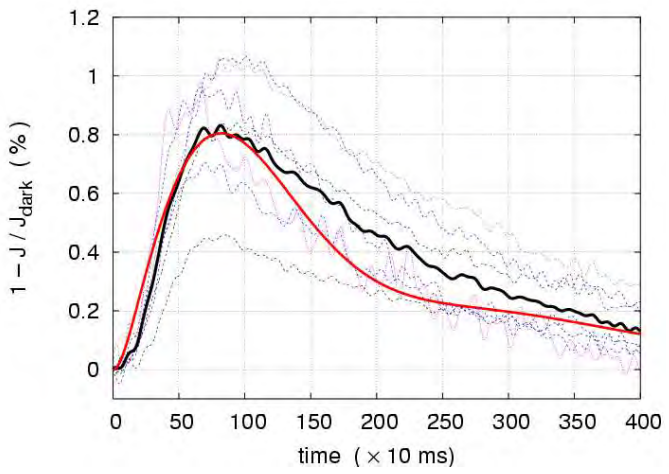

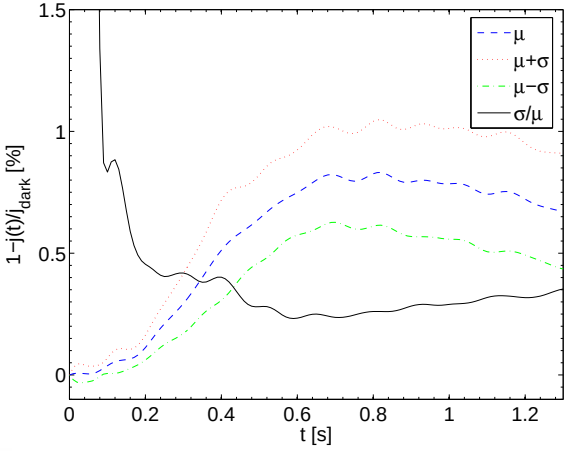

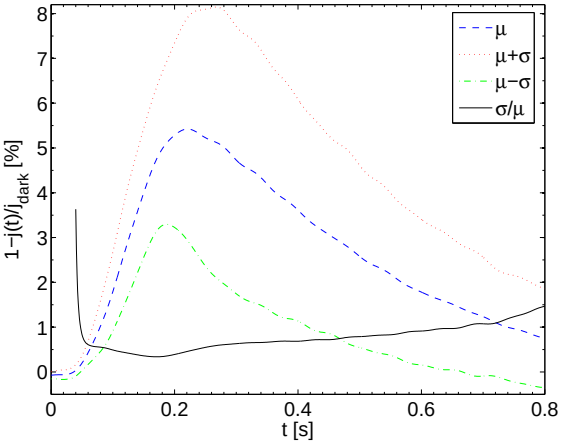

- **Left Panel:** Experimental SPR responses for Salamander (F. Rieke). Each curve is the average of a few hundred experiments. Thick black curve is their average. Red curves are simulations.

The Activation/Deactivation Cascade, Variability and Fidelity of the SPR

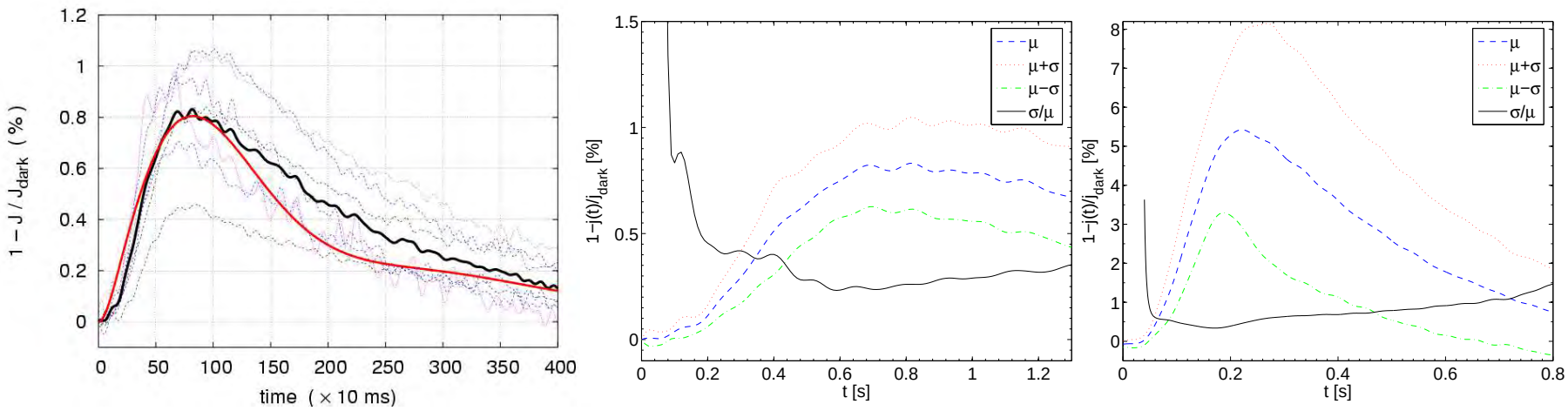

- **Left Panel:** Experimental SPR responses for Salamander (F. Rieke). Each curve is the average of a few hundred experiments. Thick black curve is their average. Red curves are simulations.
- Coefficient of Variation $CV=\sigma/\mu$; standard deviation σ over the mean μ

The Activation/Deactivation Cascade, Variability and Fidelity of the SPR

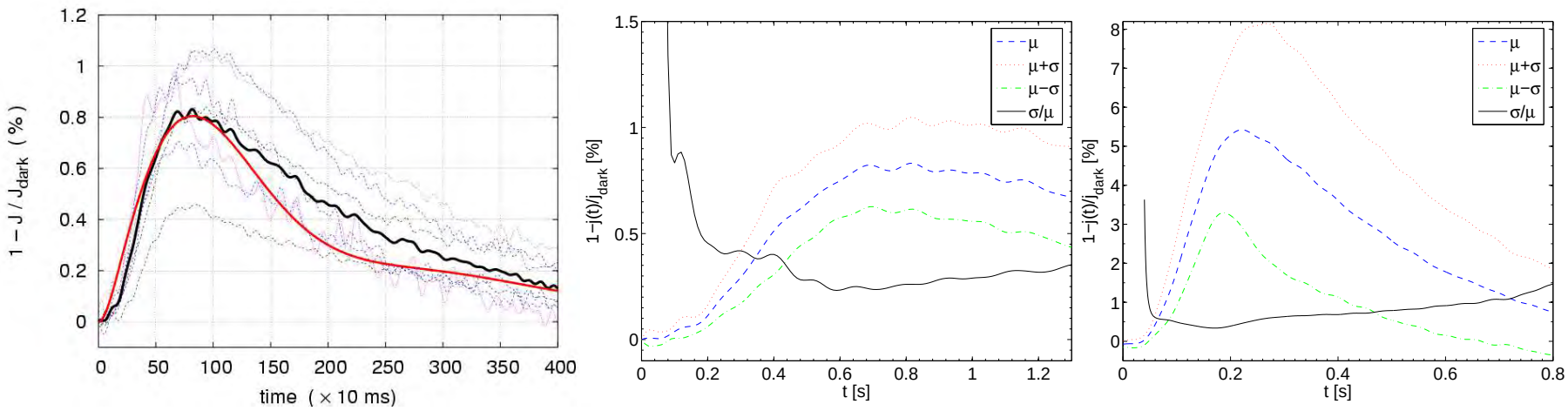

- **Left Panel:** Experimental SPR responses for Salamander (F. Rieke). Each curve is the average of a few hundred experiments. Thick black curve is their average. Red curves are simulations.
- Coefficient of Variation CV=σ/μ; standard deviation σ over the mean μ
- **Center Panel:** Experimental CV for the Salamander SPR (Rieke)

The Activation/Deactivation Cascade, Variability and Fidelity of the SPR

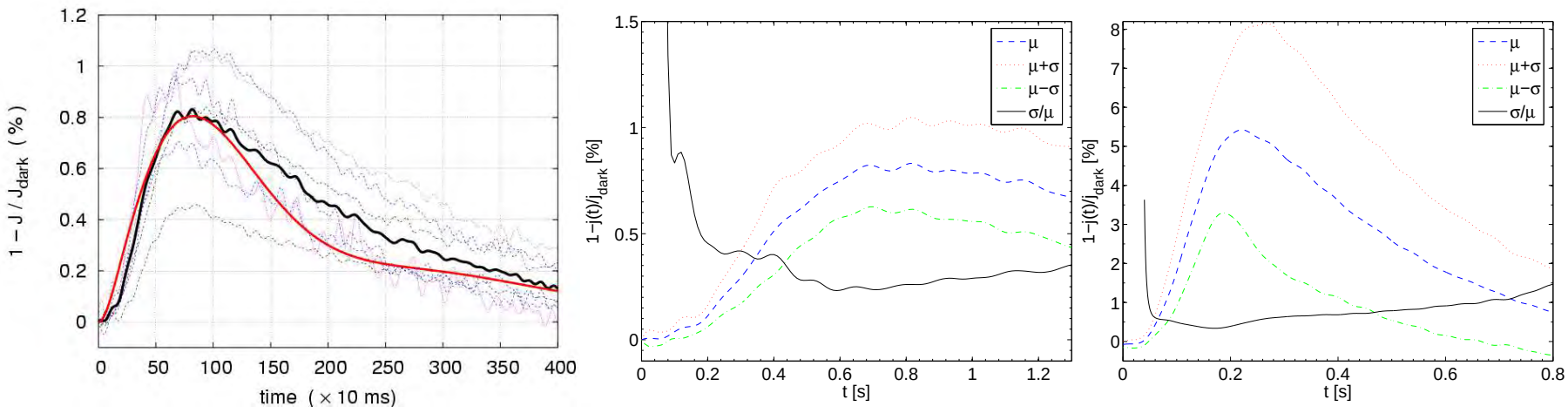

- **Left Panel:** Experimental SPR responses for Salamander (F. Rieke). Each curve is the average of a few hundred experiments. Thick black curve is their average. Red curves are simulations.
- Coefficient of Variation CV=σ/μ; standard deviation σ over the mean μ
- **Center Panel:** Experimental CV for the Salamander SPR (Rieke)
- **Right Panel:** Experimental CV for the Mouse SPR (Rieke)

The Activation Cascade and Quenching

The Activation Cascade and Quenching

- A molecule of rhodopsin, upon activation at some random location $\mathbf{x}_o$, follows its random path $t \to \mathbf{x}(t)$ in D_{eff} and becomes inactivated abruptly after a random time t_R, of average τ_R.

The Activation Cascade and Quenching

- A molecule of rhodopsin, upon activation at some random location $\mathbf{x}_o$, follows its random path $t \to \mathbf{x}(t)$ in D_{eff} and becomes inactivated abruptly after a random time t_R, of average τ_R.
- During the random interval $[0, t_R)$ R^* undergoes n molecular states R_j^*, $j = 1, \ldots, n$, each with transducer-activation rate ν_j.

The Activation Cascade and Quenching

- A molecule of rhodopsin, upon activation at some random location $\mathbf{x}_o$, follows its random path $t \to \mathbf{x}(t)$ in D_{eff} and becomes inactivated abruptly after a random time t_R, of average τ_R.
- During the random interval $[0, t_R)$ R^* undergoes n molecular states R_j^*, $j = 1, \ldots, n$, each with transducer-activation rate ν_j.
- For example R_j^* might be the phosphorylated states of R^*, identified by the number j of phosphates attached to R^* by RK. The state $(n+1)$ is identified with R^* quenching.

The Activation Cascade and Quenching

- A molecule of rhodopsin, upon activation at some random location $\mathbf{x}_o$, follows its random path $t \to \mathbf{x}(t)$ in D_{eff} and becomes inactivated abruptly after a random time t_R, of average τ_R.
- During the random interval $[0, t_R)$ R^* undergoes n molecular states R^*_j, $j = 1, \ldots, n$, each with transducer-activation rate ν_j.
- For example R^*_j might be the phosphorylated states of R^*, identified by the number j of phosphates attached to R^* by RK. The state $(n+1)$ is identified with R^* quenching.
- The transitions from the state j to $(j+1)$ occurs at some random time $0 < t_j \leq t_n = t_R$ where $t_o = 0$.

Variability Versus Biochemistry

Variability Versus Biochemistry

- If $CV \approx 1/\sqrt{n}$ (Poisson statistics), then one needs about 20 Biochemical steps to quenching

Variability Versus Biochemistry

- If $CV \approx 1/\sqrt{n}$ (Poisson statistics), then one needs about 20 Biochemical steps to quenching
- The Biochemistry says that there are only 6 phosphorylation sites on the C-terminus of the rhodopsin

Variability Versus Biochemistry

- If $CV \approx 1/\sqrt{n}$ (Poisson statistics), then one needs about 20 Biochemical steps to quenching
- The Biochemistry says that there are only 6 phosphorylation sites on the C-terminus of the rhodopsin
- How to solve the puzzle ?

Variability Versus Biochemistry

- If $CV \approx 1/\sqrt{n}$ (Poisson statistics), then one needs about 20 Biochemical steps to quenching
- The Biochemistry says that there are only 6 phosphorylation sites on the C-terminus of the rhodopsin
- How to solve the puzzle ?
- **Pugh, E. N. Jr.**, Variability of Single Photon Responses: A Cut in the Gordian Knot of Rod Phototransduction ? **Neuron, 1999, 23:205–208**

Vision-V

- **Interplay Between Stochastic and Deterministic Processes. Both are Present Essentially Always**
- **(subtitle) Analyze Randomness by Knowing the Biochemistry**
- **(subtitle) Again System Biology**

Choosing a Biochemistry

Choosing a Biochemistry

- Phosphorylation of rhodopsin by RK is a cooperative process, i.e., the incorporation of one or two phosphates increases the probability of further phosphorylation.
- The catalytic activity of R^* decreases with increasing levels of phosphorylation, at a rate of about 12% for each additional level of phosphorylation.
- **V. Gurevich**, The Selectivity of Visual Arrestin for Light-Activated Rhodopsin is Controlled by Multiple Non-Redundant Mechanisms, *J. Biol. Chem*, **1998**, *15501–15506*.

Continuous Time Markov Chain (CTMC): Variability and Biochemistry

Continuous Time Markov Chain (CTMC): Variability and Biochemistry

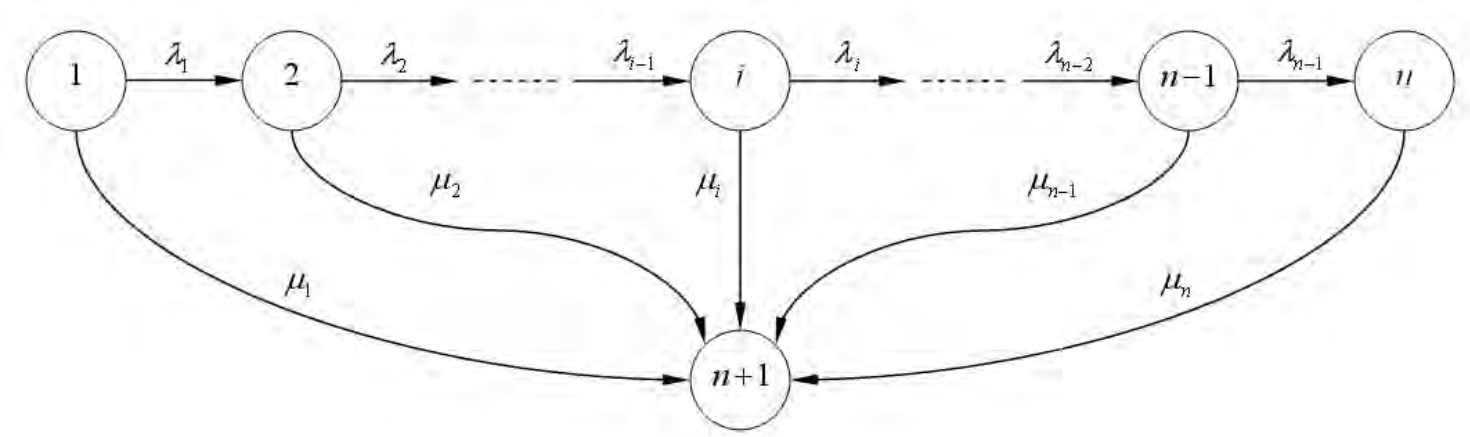

Continuous Time Markov Chain (CTMC): Variability and Biochemistry

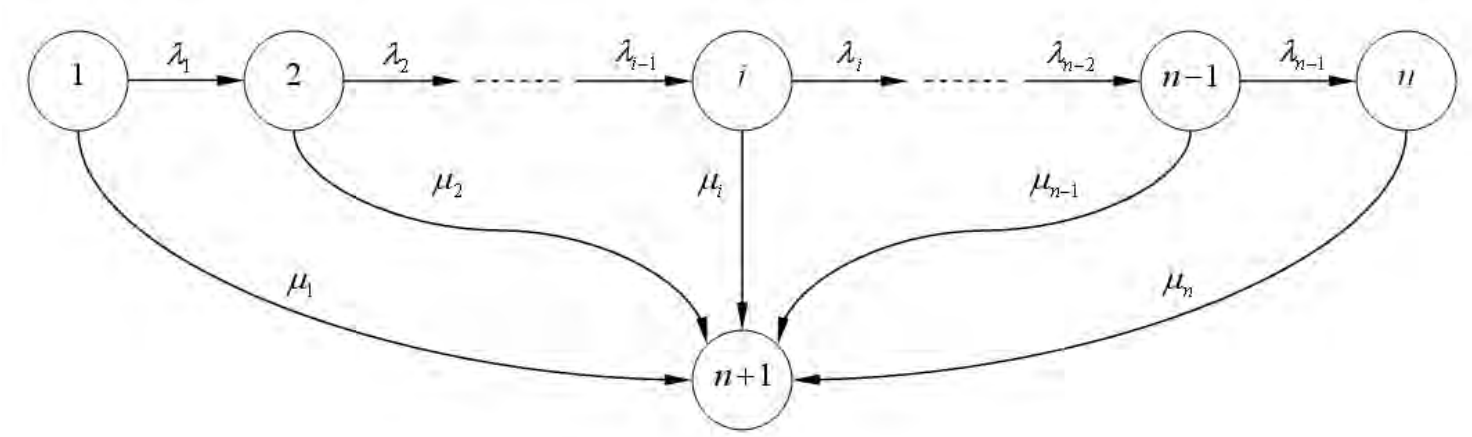

Here λ_j are affinities to phosphorylation and μ_j are affinities to Arrestin (Arr). Bernoulli process with probabilities $\frac{\lambda_j}{\lambda_j+\mu_j}$ and $\frac{\mu_j}{\lambda_j+\mu_j}$.

Continuous Time Markov Chain (CTMC): Variability and Biochemistry

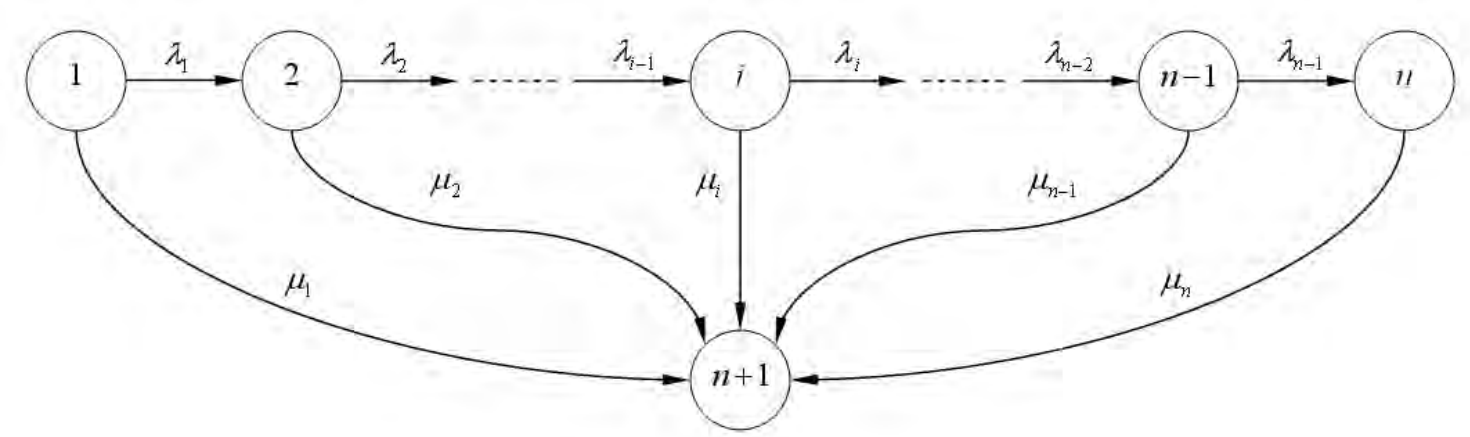

Here λ_j are affinities to phosphorylation and μ_j are affinities to Arrestin (Arr). Bernoulli process with probabilities $\frac{\lambda_j}{\lambda_j+\mu_j}$ and $\frac{\mu_j}{\lambda_j+\mu_j}$.

The λ_j and μ_j represent the Biochemistry of Deactivation.

Simulations and Functionals

Simulations and Functionals

Random events are **(a)** Activation site, **(b)** Brownian path of R^*, **(c)** Shutoff of R^* in n random steps.

Simulations and Functionals

Random events are **(a)** Activation site, **(b)** Brownian path of R^*, **(c)** Shutoff of R^* in n random steps. A sample of the Variability Functionals:

$I^*(t)$ total current up to time t

$\mathrm{E}^{**}(t)$ total activity of [PDE^*] up to time t

Simulations and Functionals

Random events are **(a)** Activation site, **(b)** Brownian path of R^*, **(c)** Shutoff of R^* in n random steps. A sample of the Variability Functionals:

$I^*(t)$ total current up to time t

$E^{**}(t)$ total activity of [PDE^*] up to time t

Main issue is:

- Why is the CV of the photocurrent low ?

Simulated and Experimental CV($= \sigma/\mu$) of Current Drop

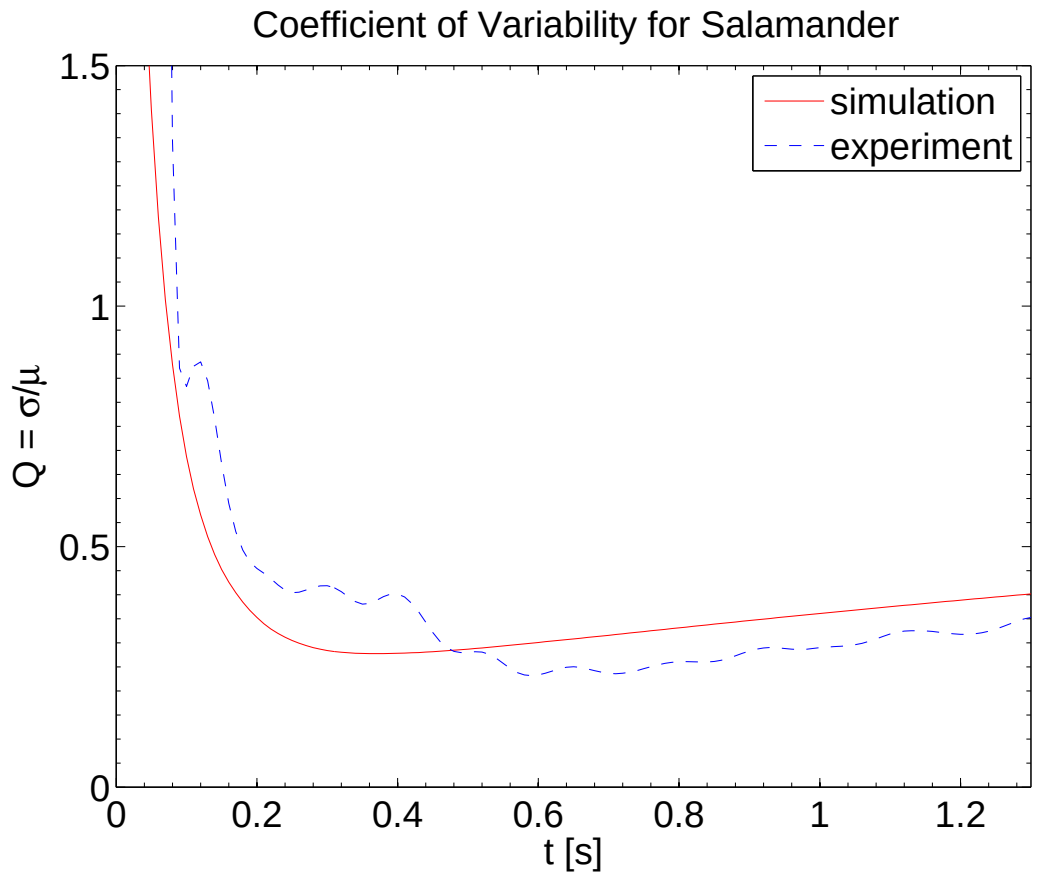

Initial instability due to Incisures; up to 32 for the Salamander, and only 1 for Mouse

Simulated CV($= \sigma/\mu$). Mouse

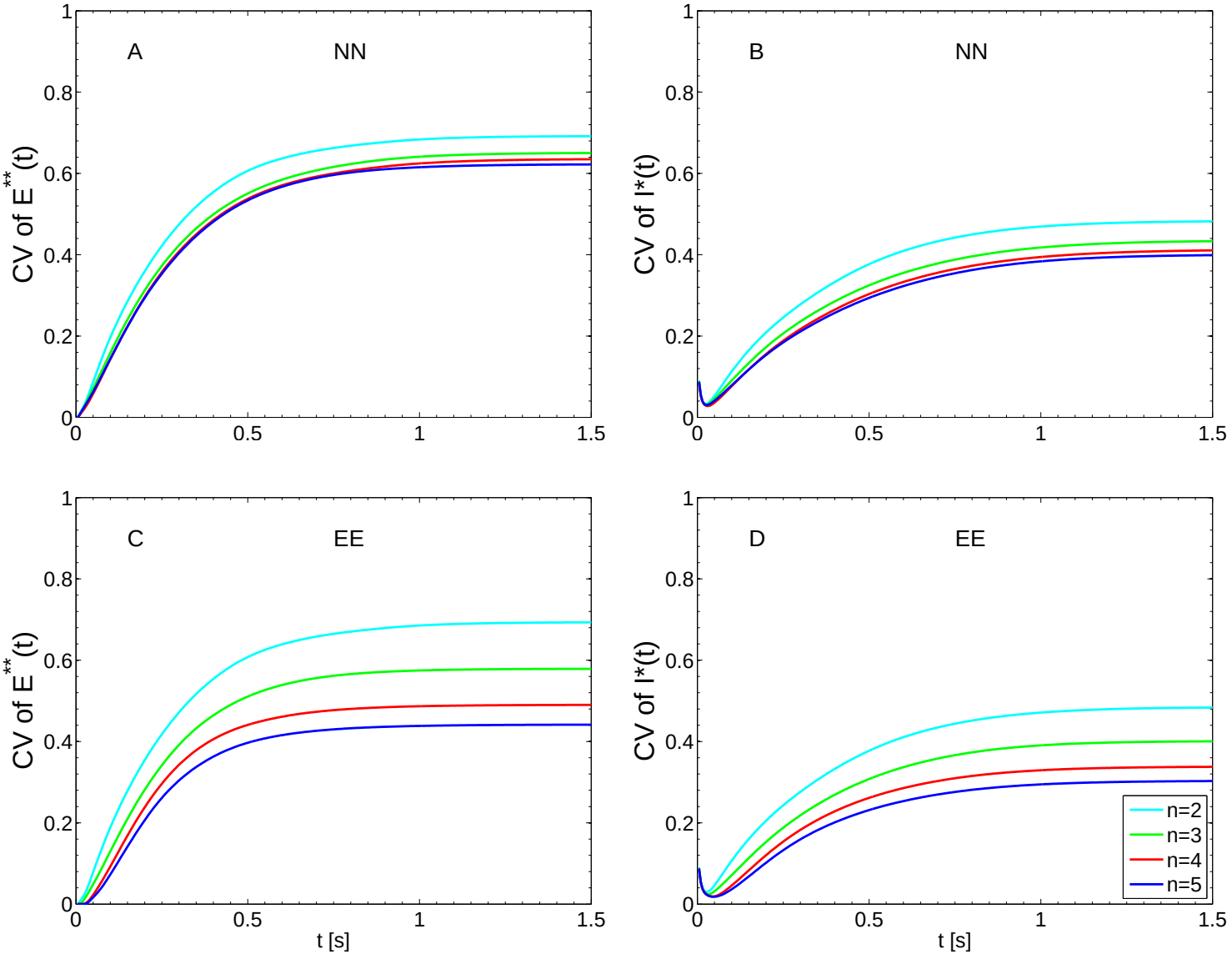

Simulated CV($= \sigma/\mu$). Salamander

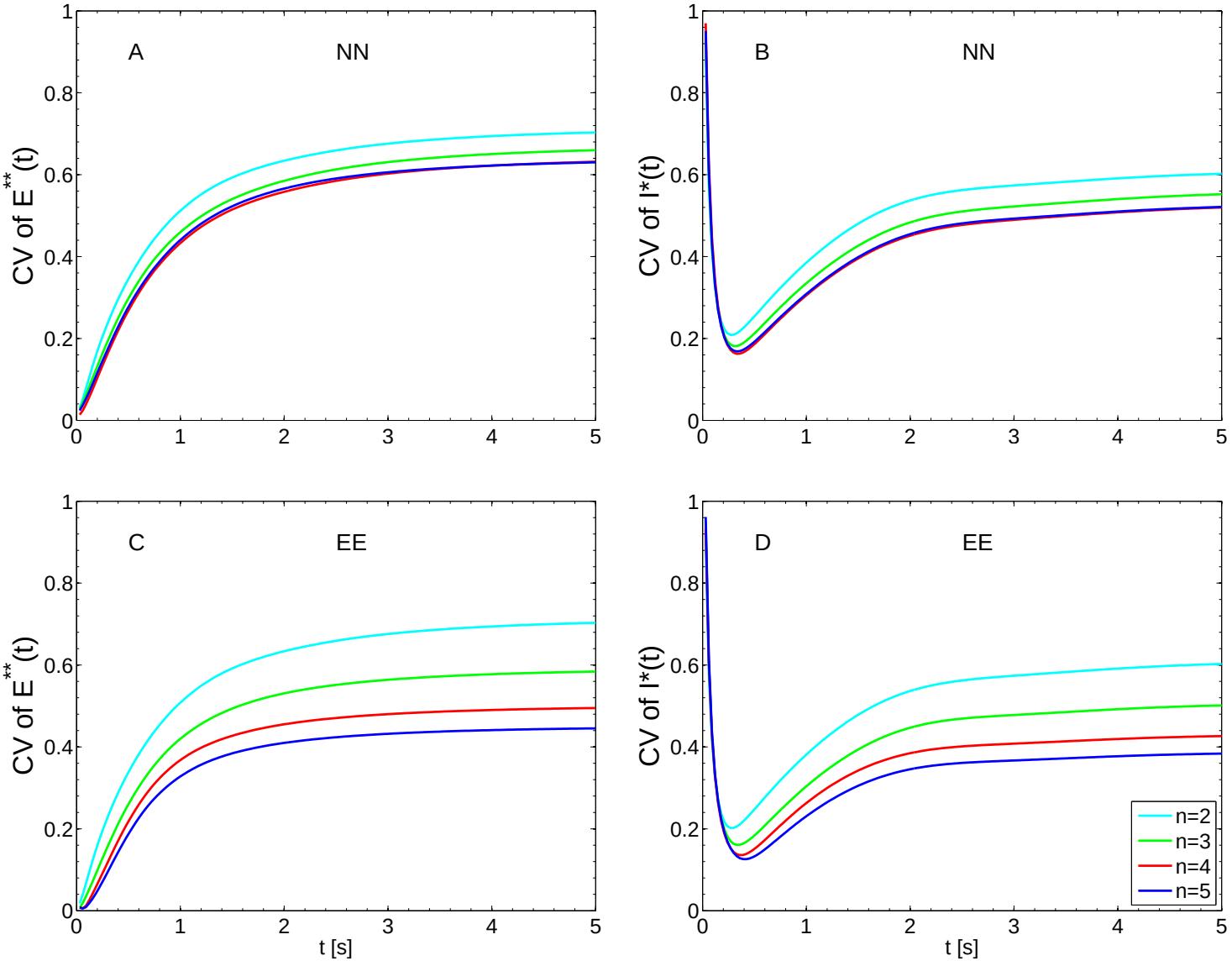

Conclusions

- Homogenization and Concentrated Capacity permits one to extract functional properties of the cell architecture. In particular:

Conclusions

- Homogenization and Concentrated Capacity permits one to extract functional properties of the cell architecture. In particular:
  - Permits one to identify the role of the incisures; an open issue in Biology up to now since they are not accessible to experiments.

Conclusions

- Homogenization and Concentrated Capacity permits one to extract functional properties of the cell architecture. In particular:
  - Permits one to identify the role of the incisures; an open issue in Biology up to now since they are not accessible to experiments.
  - Separates the process into **activation** and **diffusion of the second messengers cGMP and Ca^{2+} in the cytoplasm**. These are, as single modules, not accessible to experiments.

Conclusions

- Homogenization and Concentrated Capacity permits one to extract functional properties of the cell architecture. In particular:
  - Permits one to identify the role of the incisures; an open issue in Biology up to now since they are not accessible to experiments.
  - Separates the process into **activation** and **diffusion of the second messengers cGMP and Ca^{2+} in the cytoplasm**. These are, as single modules, not accessible to experiments.
- Analysis of the Activation cascade and experimental results, drive the choice of the Biochemistry of the shutoff mechanism of the receptor. They also permit to separate the CV of the activation stage and that of the photocurrent. In particular:

Conclusions

- Homogenization and Concentrated Capacity permits one to extract functional properties of the cell architecture. In particular:
  - Permits one to identify the role of the incisures; an open issue in Biology up to now since they are not accessible to experiments.
  - Separates the process into **activation** and **diffusion of the second messengers cGMP and Ca^{2+} in the cytoplasm**. These are, as single modules, not accessible to experiments.
- Analysis of the Activation cascade and experimental results, drive the choice of the Biochemistry of the shutoff mechanism of the receptor. They also permit to separate the CV of the activation stage and that of the photocurrent. In particular:
  - CV is high at the activation stage

Conclusions

- Homogenization and Concentrated Capacity permits one to extract functional properties of the cell architecture. In particular:
  - Permits one to identify the role of the incisures; an open issue in Biology up to now since they are not accessible to experiments.
  - Separates the process into **activation** and **diffusion of the second messengers cGMP and Ca^{2+} in the cytoplasm**. These are, as single modules, not accessible to experiments.
- Analysis of the Activation cascade and experimental results, drive the choice of the Biochemistry of the shutoff mechanism of the receptor. They also permit to separate the CV of the activation stage and that of the photocurrent. In particular:
  - CV is high at the activation stage
  - CV is suppressed by the diffusion of the second messengers cGMP and Ca^{2+}

Some Bibliography

- (with P.Bisegna, G.Caruso, D.Andreucci, L. Shen, S. Gurevich and H.E.Hamm) Diffusion of the Second Messengers in the Cytoplasm Acts as a Variability Suppressor of the Single Photon Response in Vertebrate Phototransduction, *Biophysical Journal*, **94***(9), (2008), 3363–3384.*
- (with P.Bisegna, G.Caruso, D.Andreucci, L. Lenoci, S. Gurevich and H.E.Hamm) Kinetics of Rhodopsin Deactivation and its Role in Regulating Recovery and Reproducibility in Rod Photoresponse *PLoS Comp. Biology* **6***(12), (2010), 1-15.*
- (with P.Bisegna, G.Caruso, D.Andreucci, L. Lenoci, S. Gurevich and H.E.Hamm) Identification of the Key Factors that Reduce the Variability of the Single Photon Response, *PNAS*, **108(19), 2011**, *7804–7807*.

Acknowledgments

- Daniele Andreucci, Univ. of Rome, La Sapienza, Italy
- Paolo Bisegna, Univ of Rome, Tor Vergata, Italy
- Giovanni Caruso, CNR and Univ. of Rome, Tor Vergata, Italy
- Seva Gurevich, Vanderbilt, Pharmacology
- Heidi E. Hamm, Vanderbilt, Pharmacology
- Fred Rieke (HHMI), Physiology and Biophysics, Seattle WA
- Clint Makino, Harvard Med. School, Boston MA
- Ralf Mueller, Vanderbilt, Pharmacology.
- Lixin Shen, Biomathematics Study Group, Vanderbilt.
- **Support:** NIH-1-RO1-GM 68953-01; NAS-Keck Foundation
- **Web site: http:abcd.math.vanderbilt.edu/˜signaltr/**

Vision-VI

- **Parameter Determination is an Art of its Own**
- **However .... Beware of Parameter Fitting**